Heliyon

Research article

Modeling vegetative vigour in grapevine: unraveling underlying mechanisms

Inés P. Hugalde [a,b,*], Cecilia B. Agüero [b], Felipe H. Barrios-Masias [b,c], Nina Romero [b], Andy Viet Nguyen [b], Summaira Riaz [b], Patricia Piccoli [e], Andrew J. McElrone [b,d], M. Andrew Walker [b], Hernán F. Vila [a,1]

[a] Estación Experimental Agropecuaria Mendoza, INTA, San Martín 3853, M. Drummond, 5507, Mendoza, Argentina
[b] Dept. Viticulture and Enology, UC Davis, One Shields Ave, Davis, CA 95616, USA
[c] Dept. Agriculture, Veterinary and Rangeland Sciences, University of Nevada, Reno, Reno, NV 89557, USA
[d] USDA-ARS, Davis, CA, 95616, USA
[e] Instituto de Biología Agrícola de Mendoza, UNCuyo – CONICET, Argentina

ARTICLE INFO

ABSTRACT

Mechanistic modeling constitutes a powerful tool to unravel complex biological phenomena. This study describes the construction of a mechanistic, dynamic model for grapevine plant growth and canopy biomass (vigor). To parametrize and validate the model, the progeny from a cross of Ramsey (*Vitis champinii*) × Riparia Gloire (*V. riparia*) was evaluated. Plants with different vigor were grown in a greenhouse during the summer of 2014 and 2015. One set of plants was grafted with Cabernet Sauvignon. Shoot growth rate (b), leaf area (LA), dry biomass, whole plant and root specific hydraulic conductance (k_H and L_{pr}), stomatal conductance (g_s), and water potential (Ψ) were measured. Partitioning indices and specific leaf area (SLA) were calculated. The model includes an empirical fit of a purported seasonal pattern of bioactive GAs based on published seasonal evolutionary levels and reference values. The model provided a good fit of the experimental data, with R = 0.85. Simulation of single trait variations defined the individual effect of each variable on vigor determination. The model predicts, with acceptable accuracy, the vigor of a young plant through the measurement of L_{pr} and SLA. The model also permits further understanding of the functional traits that govern vigor, and, ultimately, could be considered useful for growers, breeders and those studying climate change.

1. Introduction

Vigor is the propensity to assimilate, store, and/or use non-structural carbohydrates for producing large canopies, and it is associated with intense metabolism and fast shoot growth (Ollat et al., 2003; Rebolledo et al., 2015). Understanding vigor in grapes is necessary to optimize vineyard management and grape breeding strategies, since a vine needs enough canopy and growth to ripen the grapes. For our purposes, vigor is represented by canopy biomass. Photosynthesis (A) is the ultimate source of carbohydrates that drives plant growth. For A to occur, CO_2 must diffuse into the leaf mesophyll, through the stomata, which in turn results in H_2O molecules escaping from the leaf to the atmosphere. This inevitable water loss through the stomata (and the depreciable diffusing through cuticle), constitutes transpiration (E). This means that A and

stomatal conductance (g_s) are tightly correlated (Wong et al., 1979), and stomata are directly responsible for optimizing E *vs.* A (Rogiers et al., 2012).

At the cellular level, growth involves expansion and division (Polymenis and Schmidt, 1997). Cell expansion occurs because cell walls are extensible, meaning they deform under the action of tensile forces, generally caused by turgor (Cosgrove, 2005). Canopy hydration and turgor maintenance depend on the root system capacity for water uptake (hydraulic conductance, k_H) to meet water demands (E). This means that root k_H affects the hydration and turgor of the canopy (De Herralde et al., 2006; Lovisolo et al., 2008), resulting in different levels of cellular extension and plant growth (Di Filippo and Vila, 2011). Lower k_H has been observed in shoots grafted onto dwarfing rootstocks (Syvertsen and Graham, 1985; Atkinson et al., 2003) and in non-grafted, low vigor,

* Corresponding author.
  E-mail address: hugalde.ines@inta.gob.ar (I.P. Hugalde).
[1] Deceased author.

cherry plants (Zorić et al., 2012). This can be explained by the equation of water potential components $\Psi_p = \Psi_L\text{-}\Psi_\pi$; and the Van den Honert equation, $\Psi_L = \Psi_{soil}\text{-}(E/k_H)$; that state that turgor water potential (Ψ_p) depends on leaf water potential (Ψ_L) and osmotic water potential (Ψ_π), and that Ψ_L inversely depends on k_H. Thus, Ψ_p can be directly impacted by changes in k_H. In this way, Ψ_L increases with higher k_H, and results in higher leaf turgor (Ψ_p) and cell expansion (Fan et al., 2012). However, if k_H decreases, as result of decreasing soil moisture and cavitation (Chaves et al., 2003), or decrease in aquaporin activity (Ehlert et al., 2009; Vandeleur et al., 2009; Gambetta et al., 2012); a series of signals may reduce stomatal conductance in the leaves and decrease transpiration rates. According to the mechanistic model of stomatal closure of Buckley et al. (2003), there is a hydraulic feedback signal between gs and k_H through the regulation of the turgor potential of the guard cell, in response to variations in Ψ_L. This happens because the guard cells directly respond to the epidermal turgor potential (Ψ_p) (Chaves et al., 2003), which in turn depends on plant k_H, so reductions in k_H can be translated into reductions in g_s (Lovisolo et al., 2010; Zufferey and Smart, 2012; Pou et al., 2013).

Many hydraulic and metabolic processes are controlled or influenced by hormones, with gibberellins (GAs) being the primary hormones that control growth and development in plants (Huerta et al., 2008). Gibberellins are tetracyclic diterpenoid acids involved in a number of developmental and physiological processes in plants (Crozier et al., 2000). Among many effects, GAs activate cell division and control cell elongation (Huerta et al., 2008; Ubeda-Tomás et al., 2009), thus controlling shoot growth (amount and direction; Clúa et al., 1996). They also play an important role in regulating net photosynthesis (Huerta et al., 2008), chlorophyll degradation (Li et al., 2010), and carbohydrate production and partitioning (Lambers et al., 1995, 2008; Moreno et al., 2011; Murcia et al., 2016). However, from the +130 of GA structures characterized up to now (http://www.plant-hormones.info/gainfo.asp), only C19 3-ß and 13-∞ hydroxylated chemical forms, GA1, GA3, GA4, GA7 are active *per se* (Kobayashi et al., 1994). High purported concentrations of bioactive GAs have been proposed as responsible for heterosis in plants (Bate et al., 1988; Rood et al., 1988) and therefore to benefit canopy growth, while low concentrations of bioactive GAs benefit root biomass production. The concentration of bioactive GAs in each tissue depends on the organ analyzed, the plant phenology and on external and environmental stimuli. In grape leaves, the amount of GA19, a major GA not active *per se* but through its conversion to GA1 (Kobayashi et al., 1994), is about 20 ng g^{-1} (Acheampong et al., 2015). They may be site-synthesized by 3-beta oxidation from precursors of the inactive GA pool (Yamaguchi, 2008), de-conjugated from glycosylated forms (Piccoli et al., 1997; Cassan et al., 2001) or may travel from the roots to the canopy (Hooijdonk et al., 2010). In addition, GAs affect the biosynthesis and response of ethylene, and the synthesis and transport of auxins. A large number of GA mutants showing growth and development suppressions or dwarf phenotypes have demonstrated that the GA signaling complex is highly conserved in many species, like maize, rice, barley and grapevine (Ikeda et al., 2001; Boss and Thomas, 2002; Chandler et al., 2002; Muangprom and Osborn, 2004).

The surrounding environment also influences biomass production. Soil water status directly affects root hydraulics, while atmospheric humidity, water vapor pressure deficit, light and temperature will affect leaf water potential and stomatal conductance (Buckley et al., 2003; Buckley, 2005). These responses to external factors will affect the water uptake capacity of the plant, leaf gas exchange (g_s and A), hormonal regulation, tissue turgor and in consequence, plant growth.

The complexity that characterizes biomass production makes it necessary to find a method that simplifies their study. In this sense, mechanistic models constitute a valuable tool for researchers and biophysicists to study diverse biological phenomena. In contrast with empirical approaches, mechanistic models are based on biophysical/biochemical mechanisms. These models formalize a hypothesis, given that they are a possible description of the system and its performance. Each aspect of the performance of the dynamic model can be studied in any time frame. Once a model is validated, simulations are quick and inexpensive, whereas empirical models need to rely on experimental approaches (Ingalls, 2013). To date, several biophysical models have been constructed, interpreting for instance photosynthesis and stomatal conductance (Farquhar et al., 1980; Farquhar and Sharkey, 1982; Pury and Farquhar, 1997; Yin and Struik, 2009; Bagley et al., 2015; Wu et al., 2016; Pleban et al., 2020). Our paper describes the construction, parametrization and validation of a mechanistic, dynamic model for vigor using grapevine as the biological model. Examples of modeling in grapevine include studies of source sink relationships (Pallas et al., 2010), stomatal function and cavitation (Hugalde et al., 2018), rootstock control in scion transpiration (Peccoux et al., 2018), the dynamics of water transport (Zhu et al., 2018), berry growth (Zhu et al., 2019) and the significance of changing temperatures for grapevine architecture (Schmidt et al., 2019), among others. Our work considers that growth occurs when biomass is accumulated. This happens when CO_2 is assimilated by photosynthesis. Later this biomass is partitioned into canopy and roots. The canopy biomass, by turgor, is then transformed in leaf area, while the root biomass will manage water economy and transport to the whole plant. Our final objective is to elucidate the functional traits that govern vigor, understand the involved mechanisms and, ultimately, hypothesize about the practical use of this knowledge for growers, breeders and ecologists specialized in climate change.

This study is organized in four main sections. The first section, model construction, explains the theoretical development of the model based on the integration of a number of already existing models that explain several aspects of plant growth. The second section, which describes model parametrization and model validation, uses data obtained with a population from the cross Ramsey × Riparia to characterize the functions in the model and test its outputs. Ramsey (*V. champinii*) and Riparia Gloire de Montpellier (*V. riparia*) are known to confer to the scion high and low vigor, respectively and a population derived from their cross was developed to genetically characterize nematode resistance, lime and salt tolerance and ability to induce vigor (Lowe and Walker, 2006). Principal Component Analysis (PCA), led the parameterization strategy used to define the input and output variables. PCA allows the identification of the variables that most closely represent the trait, by searching the total variance in the data to reduce the original variables into a smaller set of linear combinations. This technique is mostly used as a tool in exploratory data analysis and for making predictive models. It is often used to visualize genetic distance, relatedness between populations, and for finding patterns in data of high dimension (Jolliffe and Cadima, 2016; Li and Ralph, 2018). The third section, model simulation and sensitivity analysis, explores the power of the model by predicting scenarios under different conditions. Finally, we discuss our results in the context of related works.

2. Model construction

This model conceives vigor as the result of the interaction of environment (soil and atmospheric conditions) and plant physiology (Figure 1). It integrates a number of already existing models that explain several aspects of plant growth. Stomatal conductance (g_s) is interpreted by the Buckley et al. (2003) model; leaf temperature (T_L) is expressed by the Campbell and Norman (2012) equations; osmotic water potential of the guard cell ($\Psi_{\pi g}$) is empirically expressed as in Taiz et al. (2015) and Tardieu and Simonneau (1998). Photosynthesis (A) is interpreted by the
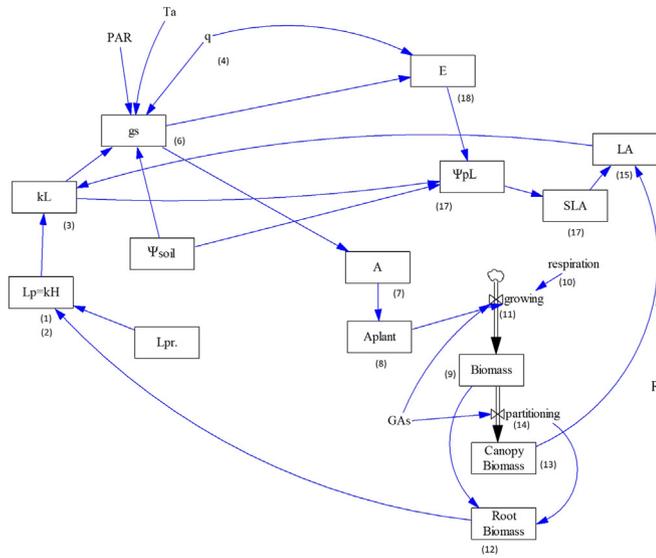
$$L_p = L_{pr} \cdot \text{root biomass} \tag{1}$$

$$k_H = L_p \tag{2}$$

$$k_L = k_H \cdot LA \tag{3}$$

$$q' = (e_{s(TL)} - e_a)/P_a \tag{4}$$

$$\Psi_{\pi g} = f(\text{solar radiation}, [ABA]) = -3 \text{ MPa} \tag{5}$$

$$g_s = \frac{X \cdot (-\Psi_{\pi g} + \Psi_{\pi e} - M \cdot \Psi_{soil} + M \cdot \Psi_{\pi e})}{1 - X \cdot (M \cdot k_L^{-1} - f_g \cdot r_g) \cdot \frac{D_b}{P_a}} \tag{6}$$

$$A = (g_s/1.6) \cdot (Ca - Ci) \tag{7}$$

$$Ca = \text{constant}$$

$$Ci = \text{constant}$$

$$\text{Aplant} = A \cdot LA \tag{8}$$

$$\text{Biomass} = (\text{Aplant} - \text{Respiration}) \cdot 0.648 \cdot i \cdot GAs \tag{9}$$

$$\text{Respiration} = 0.45 \cdot \text{Aplant} \tag{10}$$

$$\text{growth factor } i = f(L_{pr}) \tag{11}$$

$$\text{Root biomass} = \text{Biomass} \cdot (1 - \text{partitioning factor}) \tag{12}$$

$$\text{Canopy biomass} = \text{Biomass} \cdot \text{partitioning factor} \tag{13}$$

$$\text{partitioning factor} = j \cdot GAs \tag{14}$$

$$LA = \text{canopy biomass} \cdot SLA \tag{15}$$

$$SLA = f(\Psi_{PL}) \tag{16}$$

$$\Psi_{PL} = \Psi_{soil} - \frac{E}{k_L} - \Psi_{\pi L} \tag{17}$$

$$E = g_s \cdot q' \tag{18}$$

Figure 1. This model conceives vigor, defined as canopy dry weight (DWL + DWS), as the interaction of environment and plant physiology. Root hydraulic conductance (L_p, 1) is calculated from conductance per unit of root dry weight (L_{pr}) and root biomass (12). The L_p will then constitute a proxy of the plant hydraulic conductance (k_H; under no cavitation events, 2). This k_H, when divided by leaf area (LA, 15), will constitute the leaf specific hydraulic conductance (k_L, 3). The atmospheric mechanics are formalized by the Campbell and Norman (2012) equations of atmospheric deficit (q', 4) and guard cell osmotic water potential ($\Psi_{\pi g}$, 5), that are then included in the Buckley et al. (2003) equation for stomatal conductance (g_s, 6). Solar radiation, q' and temperature (T_L) will affect this g_s. Later, g_s, along with internal carbon (C_i) and atmospheric carbon (C_a), will determine net photosynthesis (A, 7). A affected by LA, will result in whole plant A (Aplant, 8), that will stoichiometrically be transformed in carbohydrates and plant biomass (9), after respiration (10) is deducted from Aplant. Specific leaf area, (SLA, 16) theoretically depends on leaf turgor (Ψ_{pL}, 17), but for our purpose, SLA is an input value dependent on the genotype that affects LA. Finally, root biomass and canopy biomass (12 and 13) will be obtained affecting the plant biomass by a factor j dependent on GAs concentration in the tissues (14). GAs also affect growth by modifying biomass with a growth factor i (11). The model has two feedback loops. At time t^{-1}, LA will be defined by canopy biomass and SLA. Later, at time t, LA will define Aplant that will again define biomass and canopy biomass, restarting the cycle. The same happens with L_p, that at time t^{-1}, defines k_H, that later defines g_s, A and biomass. This biomass will re-define L_p at time t.

Farquhar model (Farquhar et al., 1980), and biomass production is obtained by the stoichiometric equation that transforms CO_2 in carbohydrates and deducts respiration (Salisbury and Ross, 2000).

Soil water status directly affects root hydraulics and plant water status. Root hydraulic conductance (L_p, Equation (1)) depends on specific root hydraulic conductance (L_{pr},) and root biomass. L_p constitutes a proxy to plant hydraulic conductance under no cavitation events (k_H, Equation (2)). Specific hydraulic conductance (k_L, Equation (3)) is estimated from dividing k_H by leaf area (LA).

$$L_p = L_{pr} \cdot \text{root biomass} \tag{1}$$

$$k_H = L_p \tag{2}$$

$$k_L \approx k_H/LA \tag{3}$$

Atmospheric variables are formalized by the Campbell and Norman (2012) equations of atmospheric deficit (q', Equation (4)) and guard cell osmotic potential ($\Psi_{\pi g}$, Equation (5)), which depend on temperature and solar radiation, respectively. Since the purpose of the model is to simulate growth day by day, $\Psi_{\pi g}$ is considered constant and equal to -3 MPa. This value corresponds to the average daily value of the linear fit of $\Psi_{\pi g}$ and osmolites ($K+$ and sucrose) that control stomatal aperture during a complete day (Talbott and Zeiger, 1996, 1998). Equation (4) expresses the difference in density of water vapor between air (ea) and leaf (es(TL)), which is the driving force for transpiration. These variables are then included in the Buckley (2005) equation for g_s (eq. 6). An exhaustive list of the variables, their symbols and units, included in the model, and in each equation listed in Table 1.

$$q' = (e_{s(T_L)} - e_a)/P_a \tag{4}$$

$$\Psi_{\pi g} = f(\text{solar radiation}, [ABA]) = -3 \text{ MPa} \tag{5}$$

$$g_s = \frac{X \cdot \left(-\Psi_{\pi g} + \Psi_{\pi e} - M.\Psi_{soil} + M.\Psi_{\pi e} \right)}{1 - X \cdot \left(M.k_L^{-1} - f_g.r_g \right).q'} \tag{6}$$

This g_s, along with internal carbon dioxide (C_i) and atmospheric carbon dioxide (C_a), determine A (Equation (7)), in accordance to the classic model of Farquhar (Farquhar and Sharkey, 1982; Farquhar et al., 1980).

$$A = (g_s / 1.6) \cdot (C_a - C_i) \tag{7}$$

A affected by LA, results in whole plant photosynthesis (Aplant, Equation (8)), that is then stoichiometrically transformed in carbohydrates and plant biomass (Equation (9)), assuming 0.648 g of assimilated carbohydrates day^{-1} m^{-2} LA, and days with an average of 15 h of sunlight. This was calculated by considering that assimilation of 1 µmol of CO_2 s^{-1} m^{-2} is transformed into glucose by following $6CO_2 + 6H_2O = \text{glucose} + O_2$, and with a glucose molecular weight of 180.156 g mol-1. Respiration (Equation (10)) is deducted from Aplant prior to converting

Table 1. Model variables, their symbols and units.

Symbol	Variable	Units
A	Net photosynthesis	μmol m^{-2}s^{-1}
Aplant	Plant photosynthesis	μmol plant s^{-1}
Canopy biomass	Dry biomass of the canopy	G
Root biomass	Dry biomass of the roots	G
C_a	Atmospheric carbon dioxide	ppm
C_i	Internal carbon dioxide	ppm
q´	Water vapour pressure deficit	–
E	Transpiration	mmol H$_2$O m^{-2}s^{-1}
e_a	Atmospheric water vapour pressure	hPa
$e_{s(TL)}$	Saturated water vapour pressure at leaf temperature	hPa
g_s	Stomatal conductance	mmol H$_2$O m^{-2}s^{-1}MPa^{-1}
L_p	Root hydraulic conductance	mmol H$_2$O m^{-2}s^{-1}MPa^{-1}
L_{pr}	Specific root hydraulic conductance	mmol H$_2$O m^{-2}s^{-1}MPa^{-1}g^{-1}
k_H	Plant hydraulic conductance	mmol H$_2$O m^{-2}s^{-1}MPa^{-1}
k_{Hroot}	Root specific hydraulic conductance	mmol H$_2$O m^{-2}s^{-1}MPa^{-1}g^{-1}
k_L	Specific hydraulic conductance	mmol H$_2$O m^{-2}s^{-1}MPa^{-1}g^{-1}
LA	Leaf area	m^2
SLA	Specific leaf area	m^{2}g^{-1}
T_L	Leaf temperature	°C
T_a	Air temperature	°C
X	scaling constant for turgor-g_s	MPa
Ψ_{soil}	Soil water potential	MPa
Ψ_L	Leaf water potential	MPa
$\Psi_{\pi g}$	Osmotic water potential of the guard cell	MPa
Ψ_{PL}	Leaf pressure water potential	MPa
$\Psi_{\pi L}$	Leaf osmotic water potential	MPa
$\Psi_{\pi e}$	Epidermal cell osmotic potential	MPa
M	Epidermal mechanical advantage	–
r_g	Guard cell specific hydraulic resistance	mmol H$_2$O m^{-2}s^{-1}MPa^{-1}
f_g	Guard cell transpiration	mmol H$_2$O m^{-2}s^{-1}MPa^{-1}
GAs	Gibberellins, theoretical concentration	ng g^{-1}
P_a	Atmospheric pressure	hPa
ABA	Abcisic acid	

CO2 into carbohydrates. Biomass also depends on the concentration of bioactive GAs, as this type of hormones promotes growth by controlling cell division and expansion, as mentioned previously. We included a parametrized cell growth factor i, in the biomass equation (Equation (9)), that affects GAs and depends on L_{pr} (Equation (11)).

$$Aplant = A \cdot LA \tag{8}$$

$$Biomass = (Aplant - Respiration) \cdot 0.648 \cdot i \cdot GAs \tag{9}$$

$$Respiration = 0.45 \cdot Aplant \tag{10}$$

$$cell\ growth\ factor\ i = f(L_{pr}) \tag{11}$$

Root biomass and canopy biomass (Equation (12) and Equation (13)) are obtained by affecting biomass with a partitioning factor, that results from a constant index j, also parameterized by us, that scales with the concentration of bioactive GAs in the tissues (Equation (14)). Finally, LA (Equation (15)) is obtained by multiplying canopy biomass with specific leaf area (SLA, Equation (16)), which, in theory, depends on leaf turgor (Ψ_{PL}, Equation (17)) and transpiration (E, Equation (18)) but constitutes an input in our model, and relies on the genotype.

$$Root\ biomass = Biomass \cdot (1 - partitioning\ factor) \tag{12}$$

$$Canopy\ biomass = Biomass \cdot partitioning\ factor \tag{13}$$

$$partitioning\ factor = j \cdot GAs \tag{14}$$

$$LA = canopy\ biomass \cdot SLA \tag{15}$$

$$SLA = f(\Psi_{PL}) \tag{16}$$

$$\Psi_{PL} = \Psi_{soil} - E/k_L - \Psi_{\pi L} \tag{17}$$

$$E = g_s \cdot q´ \tag{18}$$

This dynamic model has two feedback loops. At time t^{-1}, LA (Equation (15)) is defined by canopy biomass (Equation (13)) and SLA (Equation (16)). Later, at time t, LA will define Aplant (Equation (8)) that, in turn, will re-define biomass (Equation (9)). The same happens with L_p, that initially defines k_H, which later will define g_s, A and biomass. This biomass will re-define L_p in time t. L_{pr} and SLA constitute the inputs of the model, while canopy dry biomass (or vigor) is the output. Other variables, parameters and constants used in the model and not described in this text, are listed in Table 1.

The model was constructed using Vensim software PLE for Windows 5.4d (Ventana systems Inc, Harvard, MA 01451).

3. Model parametrization and validation

3.1. Plant material

One hundred and twenty-five genotypes from the population from a Ramsey × Riparia cross were multiplied through green cuttings (Hugalde et al., 2017) in spring 2014. Each plant was grown in a 4L capacity pot, trained to a single shoot and watered daily. We studied three replicates per genotype in a greenhouse with an average temperature of 25 °C. Shoot growth rate was measured for 60 days, while, leaf area, leaf-shoot-root dry biomass, plant hydraulic conductance, stomatal conductance, and water potential were measured at the end of the experiment. Specific leaf area and root specific hydraulic conductivity were calculated at the end of the experiment. Raw data was grouped in clusters, as recommended for the analysis of large, quantitative, continuous and highly scattered data (Goshtasby, 2000; Berkhin, 2006), following the methodology of Armas (1988, Table 2). In 2015, the same experiment was repeated and the variables were measured to parametrize the model. In addition, specific root hydraulic conductance was measured in a subset of 50 genotypes that differed in growth and biomass. Each variable was assessed as described in Hugalde et al. (2017).

For model validation, woody-cuttings from 30 contrasting genotypes were selected from the set used in 2015 for parametrization. They were bench-grafted with Cabernet Sauvignon and grown in the greenhouse as described before. After losing two, 28 genotypes were effectively used. They were divided in 9 groups of increasing vigor (Table 3). For each group, the average value of the input parameters was used to run the simulations. Constants, parameters and units adopted for model fit and functioning are listed in Table 4. To obtain the predicted values, the model was run with a timeframe setting of 90 days with initial conditions defined as 0.5 g of initial biomass for all genotypes, no water stress (Ψ_{soil} = -0.01 MPa, q' = 0.03), and a temperature of 25 °C.

3.2. Measured variables

- Growth rate (b, m day^{-1}): shoot length was measured every 3 days, during the first 6 weeks. Parameters (intercept and slopes) were obtained from piece-wise lineal equations.
- Stomatal conductance (g_s, mmol H_2O m^{-2} s^{-1}): was measured in selected genotypes (40 genotypes in 2014 and 50 in 2015) using a Decagon SC-1 leaf porometer (Decagon Devices Inc., USA).
- Leaf and predawn water potential (Ψ_L and Ψ_{PD}, MPa): Ψ_L and Ψ_{PD} were measured at solar midday and predawn with a pressure chamber (PMS Instrument Company, OR, USA), according to Hsiao, 1990). Predawn water potential (Ψ_{PD}) was considered as a proxy for soil water potential (Ψ_{soil}).
- Plant hydraulic conductance (k_H, mmol m^{-2} s^{-1} M$_{Pa}^{-1}$): was calculated through the Van den Honert equation, with Ψ_{soil}, Ψ_L, and E.
- Root hydraulic conductance (L_{pr}, m$_3$ g DW^{-1} s^{-1} M$_{Pa}^{-1}$): was measured after Barrios-Masias et al. (2015), modified, with custom-made pressure chambers (PMS Instrument Company, OR, USA). Shoots were severed and the entire root systems were washed. Immediately, the root system was placed in plastic containers with deionized water inside the chamber and 1–3 cm stem was left protruding from the chamber lid. Once the system was sealed and secured, pressure was raised to 0.07 MPa and let to stabilize for 10 min. After stabilization, water exudation was measured gravimetrically by weighting a piece of dry gauze placed on top of the protruding stem for another 10 min (first cycle). Pressure flow assessments were conducted at increasing pressures of 0.1, 0.15, 0.2 and 0.25 MPa. At each step the system was stabilized for 7, 5, 5 and 3 min, respectively. Once the 5 cycles were completed, roots were removed from the chamber, pad dried and weighted. L_{pr} was calculated as the slope of the linear regression ($R_2 \geq 0.98$) obtained from the pressure–flow relationship (units: mmol s^{-1}MPa^{-1}) and the dry weight of the entire root system (g DW).

Table 2. Genotypes of the progeny of Ramsey x Riparia (population 9715) grouped according to their canopy biomass (DWL + DWS). Plants were grown in the greenhouse for 60 days before dry weights were determined. Groups are shown with alternate shading.

genotype	canopy (g)	genotype	canopy (g)	genotype	canopy (g)	genotype	canopy (g)	genotype	canopy (g)
9715–70	0.65	9715–26	6.38	9715–98	7.27	9715–43	8.43	9715–84	9.98
9715–95	0.82	9715–62	6.44	9715–20	7.29	9715–60	8.45	9715–32	9.99
9715–140	1.61	9715–128	6.45	9715–46	7.30	9715–45	8.47	9715–81	10.10
9715–100	1.65	9715–105	6.47	9715–139	7.35	9715–114	8.55	9715–108	10.10
9715–78	2.29	9715–107	6.53	Ramsey	7.35	9715–109	8.67	9715–87	10.37
9715–85	2.41	9715–111	6.56	9715–16	7.37	9715–53	8.69	9715–116	10.42
9715–1	2.80	9715–72	6.64	9715–125	7.39	9715–30	8.82	9715–118	10.45
9715–113	3.42	9715–89	6.68	9715–104	7.59	9715–76	8.84	9715–136	10.54
9715–94	3.70	9715–58	6.74	9715–49	7.61	9715–150	8.97	9715–77	10.64
9715–143	3.74	9715–106	6.77	9715–131	7.62	9715–82	9.19	9715–115	10.64
9715–33	4.01	9715–28	6.78	9715–7	7.64	9715–132	9.36	9715–126	10.73
9715–148	4.05	9715–50	6.81	9715–11	7.68	9715–44	9.44	9715–121	10.78
9715–22	4.44	9715–36	6.83	9715–96	7.68	9715–133	9.46	9715–112	10.88
9715–93	4.70	9715–10	6.84	9715–35	7.72	9715–2	9.48	9715–129	11.24
9715–23	4.77	9715–119	6.84	9715–59	7.78	9715–145	9.56	9715–25	11.38
9715–101	4.90	9715–91	6.85	9715–61	7.78	9715–80	9.58	9715–74	11.48
9715–55	5.19	9715–124	6.88	9715–47	7.80	9715–34	9.63	9715–12	11.61
9715–14	5.48	9715–5	6.95	9715–103	7.84	9715–37	9.73	9715–41	11.71
9715–79	5.71	9715–97	7.01	9715–137	7.95	9715–57	9.73	Riparia	12.08
9715–6	5.77	9715–17	7.02	9715–24	7.96	9715–40	9.81	9715–66	12.12
9715–63	6.06	9715–8	7.03	9715–73	7.96	9715–71	9.81	9715–120	12.25
9715–27	6.12	9715–68	7.04	9715–51	8.13	9715–75	9.88	9715–90	12.61
9715–141	6.18	9715–102	7.07	9715–144	8.24	9715–117	9.89	9715–39	12.74
9715–69	6.18	9715–135	7.07	9715–48	8.28	9715–149	9.92	9715–54	12.97
9715–4	6.29	9715–67	7.10	9715–13	8.30	9715–123	9.97	9715–29	13.47

Table 3. Subset of genotypes used in validation. Contrasting genotypes were grafted with Cabernet Sauvignon and grouped according to their canopy biomass (n = 28, 9 groups). Groups are shown with alternate shading. Table also shows corresponding root specific hydraulic conductance (L_{pr}) and specific leaf area (SLA).

genotype	canopy	L_{pr}	SLA
	(g)	(mmol m^{-2} s^{-1} MPa^{-1})	(m^{2}g^{-1})
9715–70	0.65	0.252	0.0309
9715–94	1.12	0.599	0.0261
9715–145	1.45	0.454	0.0244
9715–2	1.49	0.305	0.031
9715–133	1.52	0.144	0.0213
9715–93	1.56	0.344	0.0245
9715–97	1.73	1.776	0.0253
9715–55	1.76	0.916	0.027
9715–101	1.88	0.216	0.0248
9715–53	1.88	0.548	0.0269
9715–135	2.02	0.629	0.0331
9715–120	2.07	0.208	0.0247
9715–121	2.14	0.225	0.027
9715–1	2.18	0.518	0.0222
9715–72	2.33	0.351	0.0239
9715–78	2.35	0.258	0.0265
9715–99	2.71	0.614	0.0235
9715–68	2.83	0.231	0.026
9715–25	3.15	0.225	0.0258
9715–54	3.8	0.332	0.0296
9715–123	4.1	0.129	0.021
9715–115	4.21	0.174	0.0263
9715–12	4.27	0.202	0.0285
9715–4	4.3	0.475	0.0283
9715–45	4.36	0.139	0.0249
9715–44	4.78	0.533	0.0253
9715–50	5.15	0.528	0.0238
9715–57	5.7	0.611	0.0241

- Biomass (DW, g): after 60 days, leaves, shoots and roots, were dried separately at 60 °C for 72 h, to obtain their dry weights (DWL, DWS, DWR, respectively).
- Leaf area (LA, m^2): leaves were scanned with a LI-3100C Area Meter (LiCOR Inc.).
- Specific Leaf Area (SLA, m^2 g^{-1}): was calculated by dividing LA with DWL.

In addition, the pruning weights of two year-old plants growing in the UC Davis vineyard were measured in 108 genotypes of the Ramsey × Riparia population.

3.3. Parametrization

After studying the variables one by one (Figures 2 and 3), a multivariate approach was followed in order to analyze the variables and their relations. Principal Component Analyses (PCA) were conducted in 2014 and 2015 using Stat Graphics Plus 4.0 (Statistical Graphics Corp., StatSoft
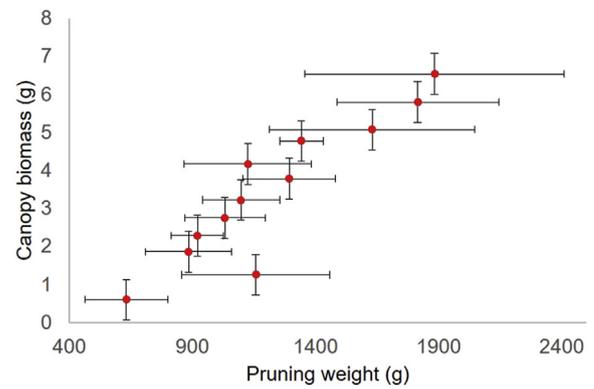

Figure 2. (a) Canopy biomass (DWL + DWS), (b) LA and (c) DWR, after grouping according to vigor (intervals of 1 g, n varies with group, total n = 125). (d) shows canopy biomass *vs.* root L_{pr} (variable n in each group; total n = 50). Bars show standard error. Genotypes ordered according to vigor are listed in Table 3.

Inc., 2003). The PCA was able to explain 80% of the variability by its two first components. Component 1, accounting for 52.5% of total variability, showed strong positive effects of LA, growth rate (b), DWL and DWR, while strong and negative effect of L_{pr} (Figure 4). This negative effect shows that in this progeny, more vigor corresponds to lower L_{pr}, meaning that smaller plants and smaller root systems are more effective in water absorption per biomass weight than vigorous plants. However, this is compensated by DWR, making vigorous root systems, with higher dry biomass, hydraulically superior for water delivery to the canopy. For component 2, accounting for 27.5% of total variability, positive effects were explained by SLA, and the partitioning index between LA and total biomass.

The identification of the phenotyped traits that significantly correlated to vigor led the parametrization strategy through L_{pr} and SLA, the two inputs of the model, both clearly identified in the PCA. Using these input variables and adjusting the purported concentration of bioactive GAs, the model predicted the resulting vigor for each case, allowing the calculation of growth and partitioning indices i and j. The additional measured variables, e.g. E, DWR, DWL, used in the statistical analysis and PCA construction, served as model simulation controls.

For parametrization of cell growth factor i and index j, the average value of input variables L_{pr} and SLA and output variable vigor, were calculated for each group of genotypes (Table 2). Significant correlation with L_{pr} was found after analyzing the association between the obtained factor i and the variables in the model. In this way, Equation (19) (R Pearson = 0.73; p-value = 0.016), explained the relation between factor i and L_{pr}. Consequently, cell growth factor i depends on L_{pr} and is required for the calculation of biomass.

$$\text{cell growth factor i} = -2.04 \cdot L_{pr} + 0.926 \tag{19}$$

On the other hand, index j was inferred after the analysis of the relation between SLA and the residues calculated from the observed vs. predicted canopy biomass showed no fit (data not shown). It resulted in a constant equal to 0.05, which scaled partitioning with bioactive GA concentration for each time t (days of growing season).

Table 4. Constants, parameters and their units adopted for model fit and functioning. The model was run with a timeframe setting of 90 days.

C_a	C_i	Ψ_{soil}	$\Psi_{\pi g}$	T_L	e_a	j	i	X	M
ppm	ppm	MPa	MPa	°C	hPa	-	-	-	-
375	0.7*375	0.01	-3	25	3	0.05	variable	105	0.98

C_a: atmospheric carbon; C_i: internal carbon; Ψ_{soil}: soil water potential; $\Psi_{\pi g}$: osmotic water potential of the guard cell; T_L: leaf temperature; e_a: atmospheric water vapor pressure; j: Partition scaling parameter; i: Growth scaling parameter; X: scaling constant for turgor-gs (Buckley et al., 2003); M: mechanical advantage of epidermis.
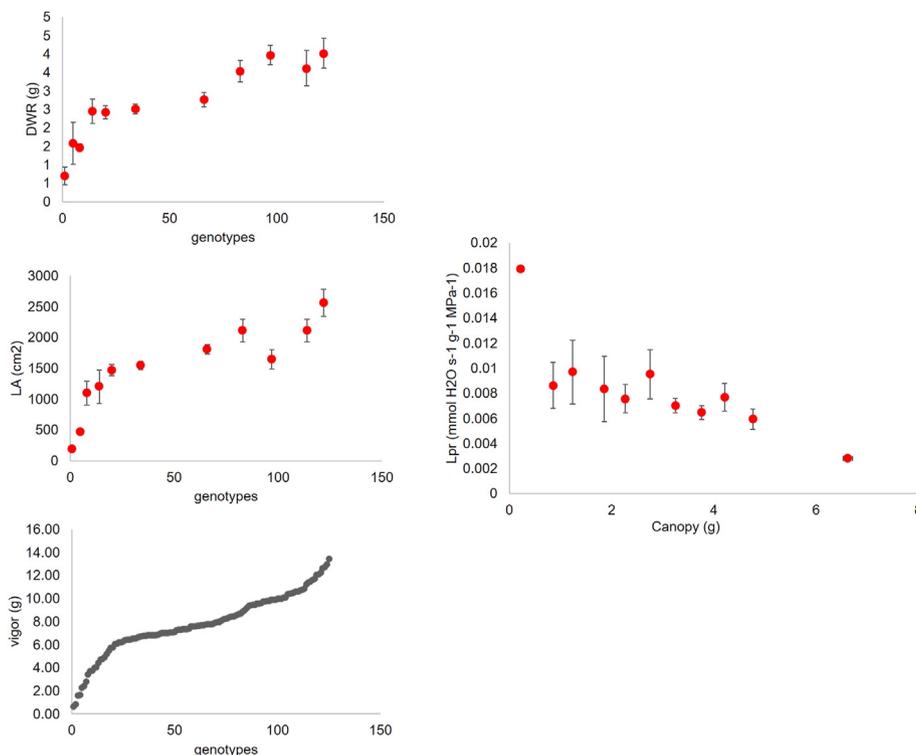
Figure 3. Canopy biomass (DWL + DWS) of 60 day old potted plants *vs.* pruning weights of two year old field plants, R Pearson = 0.91. Averages were calculated after grouping according to canopy biomass in pots (intervals of 0.5 g, n varies with group, total n = 108). Bars show standard error.

An empirical fit of the purported concentrations of bioactive GAs was calculated, based on the seasonal dynamics of some species (Kopcewicz, 1968; Yörük et al., 2004) and the measured values of leaves and buds of grapevines (Acheampong et al., 2015). The equation fit is:

$$GAs = a^{\left(\frac{(time-b)^2}{c}\right)};$$

where a: 22.27; b: 27.44; c: -1901; and time is days of a growing season.

3.4. Validation

The ability of the model to accurately estimate vigor was tested through the correlation between observed and predicted data, and by calculation of the mean-squared prediction error (MSPE), which accounts for the sum of three components, namely mean bias, line bias and random variation (Bibby and Toutenburg, 1977; Dhanoa et al., 1999). The MSPE is the expected value of the squared difference between the fitted values implied by the predictive function and the values of the (unobservable) function. The root mean square error (RMSE), represents an analogue to standard deviation, and is calculated as square root of MSPE. Statistically significant correlations (R Pearson = 0.85) were found between observed vigor and predicted values (Figure 5). In our experiment, MSPE was 5 g, and the RMSE 2.2 g, being 0.65 g the lowest value measured in the progeny and 13.47 g the highest (Table 2). The mean bias, or difference between the observed mean and predicted mean, expressed as proportion of the MSPE (mean bias/MSPE), was 0.89. This means that almost 90% of the MSPE had mean bias. A mean bias different from zero indicates that predicted values can be consistently higher or lower than the observed values. Our estimated values were consistently lower than the observed ones, indicating that the model could strongly predict which plant was bigger or smaller, by sub-estimating the final biomass. The line bias, which is the deviation of the slope of the regression line from the line of unity, scaled to MSPE (line bias/MSPE), was 0.003. Finally, the random

variation or the variability that is contained within a process that cannot be determined, scaled to MSPE (random variation/MSPE), was 0.10.

4. Model simulation and sensitivity analysis

The validation of the model allowed simulations of real vs. single variable modification scenarios that helped determine the individual effect of certain variables with respect to others. Since our model has two main plant inputs that control vigor, namely SLA and L_{pr}, plus the effect of hormone dynamics represented by GAs, we run it keeping two input variables constant while varying one. This made possible simulations of hypothetical situations that resulted in the quantification of the individual effect of the third variable as if "it was the only variable defining vigor differences".

Simulations focusing on the individual effect of L_{pr}, GAs or SLA, using values matching a vigorous plant obtained in the parametrization step,
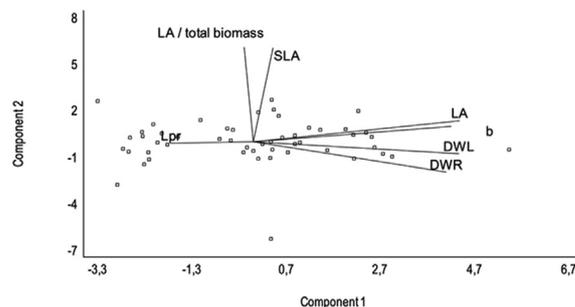

Figure 4. Principal Components Analysis of the main phenotypic traits related to vigor in 2015. L_{pr}: root specific hydraulic conductance; b: stem growth rate; SLA: specific leaf area; DWL: leaf dry weight; DWR: root dry weight; LA: leaf area; LA/total biomass: partitioning index. N = 50. Adapted from Hugalde et al. (2017). Similar results were obtained in 2014 (data not shown).
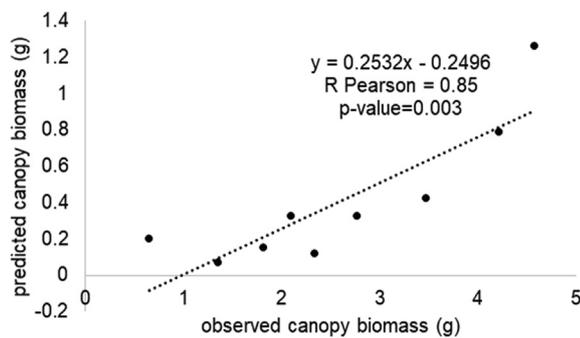
Figure 5. Observed canopy biomass (DWL + DWS) of Cabernet Sauvignon grafted onto different genotypes of the progeny of Ramsey x Riparia, *vs.* canopy predicted by the model.

showed that a big plant (high SLA, high GAs and 0.005 mmol H_2O m^{-1} s^{-1} MPa^{-1} g^{-1}) would be 42% bigger if it had the L_{pr} measured in a small plant (0.6 mmol H_2O m^{-1} s^{-1} MPa^{-1} g^{-1}) (Figure 6a). On the other side, the individual effects of purported bioactive GAs (Figure 6b) and measured SLA (Figure 6c), using values corresponding to a big plant or a small plant, while keeping the other two variables constant (high SLA and 0.005 mmol H_2O m^{-1} s^{-1} MPa^{-1} g^{-1} or high GAs and 0.005 mmol H_2O m-1 s^{-1} MPa^{-1} g^{-1}) were much stronger than that of L_{pr}. In other words, SLA and GAs play in favor of vigor in big plants, masking their less efficient water conductances. The 'compensation effect' is clearly exposed using real numbers of the three variables in the simulation (Figure 6d).

5. Discussion

In this research, we studied vigor, growth and the mechanisms involved in biomass accumulation and partitioning. We considered growth a prime topic in relation to agricultural production, the inspiration for this study. The result was the generation of a mechanistic model that integrated both chemical and biophysical mechanisms in relation to growth.

The input variables L_{pr}, SLA and purported amount of bioactive GAs were among the most important variables in defining vegetative vigor. This was proved mechanistically and is consistent with several studies demonstrating that hydraulics are related to growth and vigor (Clearwater et al., 2004; Marguerit et al., 2012; Sivasakthi et al., 2017), and that active GAs are responsible for vegetative growth (Lambers et al., 1995, 2008; Moreno et al., 2011; Murcia et al., 2016). Our model could
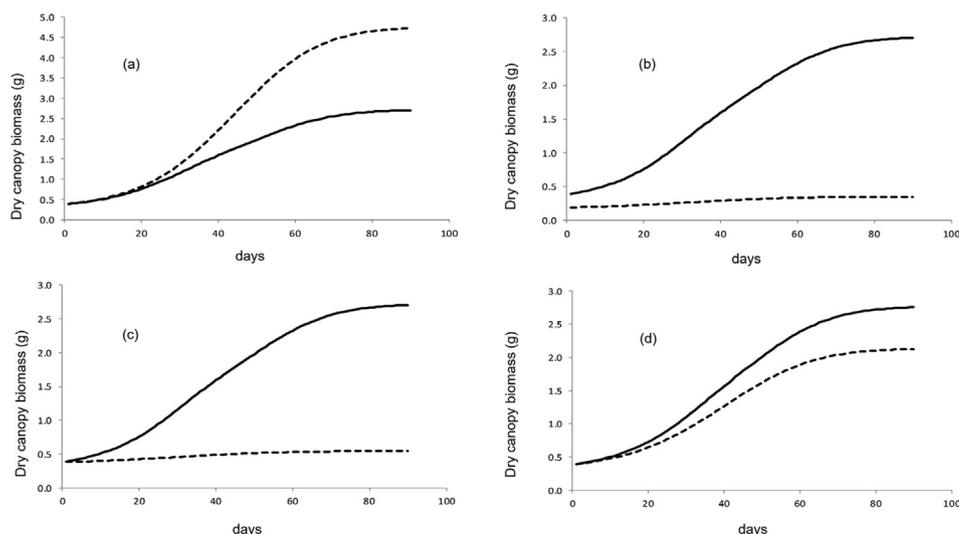
also test SLA, and explain its key role in vigor, something previously observed and measured empirically. SLA integrates both most significant vigor measurements: leaf area (LA) and leaf biomass (DWL). This variable has large physiological significance: the higher its value, the bigger the LA that will capture light for photosynthesis per unit of biomass previously synthesized. It has been shown by others that vigorous plants have higher SLA values than small plants (Reich et al., 1998; Bultynck and Lambers, 2004; Nouvellon et al., 2010; Karavin, 2014), as we confirmed with PCA analysis and our model.

The validation of our model makes it a good foundation for future theoretical and applied research. When a theoretical model is validated, it becomes not only an accepted hypothesis, but also an important prediction tool, providing a quicker, confident and low-cost experimental foundation for studying specific phenomena (Fourcard et al., 2008; Ingalls, 2013). Our validated model can help study plant growth and development in an easier and less expensive way than the traditional empirical experiment-based methodology. The fact that the model includes key environmental variables that modulate plant physiology, permits to imagine virtual experiments assessing, for instance, plants response to vineyard management practices (i.e. irrigation, shoot thinning, leaf removal, etc.), or even climate change effects on plant growth (i.e., temperature, humidity, water availability, radiation, etc.).

The model correctly estimates relative plant size, but the fact that it consistently sub-estimates vigor, should be studied and improved by a fine scaling parametrization. Another characteristic to be observed is that the model does not consider the possible effects of interactions within the canopy because it was developed in plants trained to just one stem. Also, the general nature of some of the equations does not consider aspects like plant nutrition in photosynthesis, or embolism after water scarcity in hydraulics. A future coupling with a previous cavitation model (Hugalde et al., 2018) could cover this issue. The use of L_p as a proxy for k_H is another limitation that could be addressed to refine the model, as well as more localized measurements like fine rooting. The lack of hormone measurements was partially overcome by the inclusion of an empirical equation fitting seasonal patterns of GAs previously studied in woody species and grapevines (Kopcewicz, 1968; Yörük et al., 2004; Acheampong et al., 2015). This methodology is widely accepted in modelling, since many parameters that are difficult to assess *in situ*, are often adopted from bibliography, especially in biological/molecular subjects (Magni and Saparcino, 2014; Cobelli and Carson, 2019). Peccoux et al. (2018), for example, adopted parameters from literature when including the Penman-Monteith equation to a model for rootstock control of scion transpiration in grapevine. Measurement of GAs is challenging, costly and difficult, especially because accurate measurement of specific

Figure 6. Simulations of growth for 90 days. L_{pr}: root specific hydraulic conductance; b: stem growth rate; SLA: specific leaf area; GAs: bioactive gibberellins (a): a big plant (high SLA and GAs) with high values of L_{pr}, (dotted line) and low values of L_{pr} (solid line). (b): a big plant (high SLA and low L_{pr}) with high values of GAs (solid line) and low values of GAs (dotted line). (c): a big plant (high GAs and low L_{pr}) with high values of SLA (solid line) and low values of SLA (dotted line). (d): a big plant with high SLA, high concentration of GAs and low value of L_{pr} (solid line) and a small plant with low SLA, low concentration of GAs and high value of L_{pr} (dotted line).

bioactive GAs requires sophisticated equipment and isotopically labeled internal standards (Šimura et al., 2018). An alternative to validate GAs measurements is using specific inhibitors of the synthesis of bioactive GAs, type Ca-Prohexadione. However, application of Ca-Prohexadione is phytotoxic on grapevines (R. Bottini, personal communication). Nevertheless, the patterns of seasonal changes of GAs in different species including grapevines, is quite similar (Hedden and Sponsel, 2015), providing confidence in the equation used in this model. Finally, the inclusion of empirical measurements of the model's parameters might need adjustments for other species, such as very small or very vigorous plants, trees or herbs.

Model simulations provided clarity on the individual effect of each variable that accounted for large portions of the observed variability. It also allowed us to understand the effect that some variables play over others by comparing the model situations with reality. Simulations with the model using variables from the progeny, found that SLA and GA concentration play vital roles in the development of bigger canopies and root systems with higher whole root hydraulics. In our progeny, the measured L_{pr} was lower in large plants. This may be understood as an adaptive strategy to improve their root hydraulic conductivity, *e.g.* plants with small root systems develop higher specific conductivities and plants with low specific conductivity grow larger root systems. Responses of vigor to hydraulic conductivity and its relationship with carbohydrate partitioning have been reported in other systems. For example, genetic transformation of *Arabidopsis thaliana* with an anti-sense construct targeted to the PIP1b aquaporin gene, resulted in reduced cellular water permeability that was accompanied with an increase of root mass to ensure sufficient water supply to the plant (Kaldenhoff et al., 1998). Overexpression of the same gene in tobacco improved plant vigor, transpiration rate, stomatal density, and photosynthetic efficiency under favorable conditions (Aharon et al., 2003). Also, studies in grafted kiwi plants showed that whole plant hydraulic conductance was lower but leaf-area-specific conductance (k_L) and g_s were both higher in low-vigour rootstocks (Clearwater et al., 2004). These authors suggest that changes in biomass partitioning to the roots and crown structure are involved in the observed rootstock effects. Another study with two chickpea genotypes contrasting for vigor showed that early vigor genotypes had lower root hydraulic conductivity and transpiration rates than late vigor lines (Sivasakthi et al., 2017). However, this would be compensated by their larger root system under low vapor pressure deficit conditions.

The fact that ungrafted rootstocks grow vigorously does not imply that they will confer more vigor to the scion. For example, relatively vigorous motherlines like 420A, 5C, and 101-14 perform as low vigor rootstocks, while St George, 110R, 140Ru and Ramsey are relatively weak mother vines that confer high vigor to the scions (M. Andrew Walker personal observation). The interaction between scion and rootstock has been widely studied, since the relation between both genotypes can produce varied phenotypes; and both canopy and roots must be involved in whole plant regulation (Tandonnet et al., 2010; Cookson and Ollat, 2013; Albacete et al., 2015; Miele and Rizzon, 2017). In our study, Ramsey displayed less vigor than Riparia Gloire (Hugalde et al., 2017). However, it is well documented that they are considered invigorating and devigorating rootstocks respectively. According to our model, this would imply that grafting modifies the relation between variables like L_{pr}, root biomass, etc. so that we could speculate that the higher L_{pr} displayed by Ramsey would become a main factor influencing the vigor of grafted plants. This is in accordance with a study in grapevines that showed that fine roots of invigorating and drought resistant 110R had higher L_{pr} than 101-14, a less invigorating rootstock (Barrios-Masias et al., 2015). The same was observed before by Gambetta et al. (2012), who found that invigorating rootstocks tended to have higher L_{pr} than rootstocks that conferred low vigor to the scion. In addition, Peccoux et al. (2018) found that Cabernet Sauvignon grafted onto 110R exhibited higher g_s and E than Cabernet Sauvignon grafted onto 101-14 under well-watered and moderate water deficit, probably due to the higher root length area developed by 110R. . But, shoot physiological responses of Cabernet Sauvignon grafted onto Ramsey and Riparia Gloire were similar under drought stress (Barrios-Masias et al., 2018).

It is noteworthy that in our research, model validation was achieved using 3 months old grafted plants, meaning that the model was able to predict vigor in a quite accurate manner in such a different set of plants. In the future, it might be interesting to include a parameter that incorporates grafting effects, in order to better comprehend the relationship between 2 different genotypes and their partitioning. This was not evident in our study since the plants were only 2–3 month old but could be manifested in older plants in the field.

The model allowed the assembling of the relevant functional traits that underlay vigor and the comprehension of their interactions and emerging features. We believe that our model could be the initial step in developing a practical diagnosis tool for breeders and growers. It is known that balanced vigor is crucial for grapevine production. Modeling approaches could become an instrument for analysis of crop growth, assisting vineyard management. In addition, models like the one we propose may help ecological and environmental studies address the climate change scenario we are currently facing.

6. Conclusions

The validation of the theoretical model developed for grapevine helped to identified the most important mechanisms underlying vegetative growth. It simulated growth in an acceptable manner, empowering its potential use as a prediction tool that could be applied in the fields of viticulture and ecology. Root hydraulics, theoretical hormone dynamics and specific leaf area were the key variables in our model that controlled vegetative growth. It remains necessary to measure hormones to further refine the model. However, we propose that by measuring L_{pr} and SLA in young plants, and estimating hormone impacts, our model can predict, with acceptable accuracy, the expected vigor of different genotypes.

Declarations

Author contribution statement

Inés P. Hugalde: Conceived and designed the experiments; Performed the experiments; Analyzed and interpreted the data; Wrote the paper.

Cecilia B. Agüero: Conceived and designed the experiments; Performed the experiments; Analyzed and interpreted the data; Contributed reagents, materials, analysis tools or data.

Felipe H. Barrios-Masias: Conceived and designed the experiments; Performed the experiments.

Nina Romero, Andy Viet Nguyen: Performed the experiments.

Summaira Riaz, Patricia Piccoli: Contributed reagents, materials, analysis tools or data.

Andrew J. McElrone, M. Andrew Walker, Hernán F. Vila: Conceived and designed the experiments; Analyzed and interpreted the data; Contributed reagents, materials, analysis tools or data.

Data availability statement

Data included in article/supplementary material/referenced in article.

Declaration of interests statement

The authors declare no conflict of interest.

References

Acheampong, A.K., Hu, J., Rotman, A., Zheng, C., Halaly, T., Takebayashi, Y., Jikumaru, Y., Kamiya, Y., Lichter, A., Sun, T.-P., 2015. Functional characterization and developmental expression profiling of gibberellin signaling components in *Vitis vinifera*. J. Exp. Bot. 66, 1463–1476.

Aharon, R., Shahak, Y., Wininger, S., Bendov, R., Kapulnik, Y., Galili, G., 2003. Overexpression of a plasma membrane aquaporin in transgenic tobacco improves plant vigor under favorable growth conditions but not under drought or salt stress. Plant Cell 15, 439–447.

Albacete, A., Martínez-Andújar, C., Martínez-Pérez, A., Thompson, A.J., Dodd, I.C., Pérez-Alfocea, F., 2015. Unravelling rootstock × scion interactions to improve food security. J. Exp. Bot. 66, 2211–2226.

Armas, J., 1988. Estadística Sencilla: Descriptiva. Consejo de Publicaciones de la Universidad de los Andes, Venezuela, Mérida.

Atkinson, C.J., Else, M.A., Taylor, L., Dover, C.J., 2003. Root and stem hydraulic conductivity as determinants of growth potential in grafted trees of apple (*Malus pumila* Mill.). J. Exp. Bot. 54, 1221–1229.

Bagley, J., Rosenthal, D.M., Ruiz-Vera, U.M., Siebers, M.H., Kumar, P., Ort, D.R., Bernacchi, C.J., 2015. The influence of photosynthetic acclimation to rising CO2 and warmer temperatures on leaf and canopy photosynthesis models. Global Biogeochem. Cycles 29, 194–206.

Barrios-Masias, F., Knipfer, T., McElrone, A., 2015. Differential responses of grapevine rootstocks to water stress are associated with adjustments in fine root hydraulic physiology and suberization. J. Exp. Bot. 66, 6069–6078.

Barrios-Masias, F., Knipfer, T., Walker, M.A., McElrone, A.J., 2018. Differences in hydraulic traits of grapevine rootstocks are not conferred to a common *Vitis vinifera* scion. Funct. Plant Biol. 46, 228–235.

Bate, J.B., Rood, S.B., Blake, T.J., 1988. Gibberellins and heterosis in poplar. Can. J. Bot. 66, 1148–1152.

Berkhin, P., 2006. A survey of clustering data mining techniques. In: Grouping Multidimensional Data.

Bibby, J., Toutenburg, H., 1977. Prediction and Improved Estimation in Linear Models. Wiley, Berlin, Germany.

Boss, P.K., Thomas, M.R., 2002. Association of dwarfism and floral induction with a grape 'green revolution' mutation. Nature 416, 847–850.

Buckley, T.N., Mott, K., Farquhar, G., 2003. A hydromechanical and biochemical model of stomatal conductance. Plant Cell Environ. 26, 1767–1785.

Buckley, T.N., 2005. The control of stomata by water balance. New Phytol. 168, 275–292.

Bultynck, L., Lambers, H., 2004. Effects of applied gibberellic acid and paclobutrazol on leaf expansion and biomass allocation in two *Aegilops* species with contrasting leaf elongation rates. Physiol. Plantarum 122, 143–151.

Campbell, G.S., Norman, J.M., 2012. An Introduction to Environmental Biophysics. Springer, New York, USA.

Cassán, F., Bottini, R., Schneider, G., Piccoli, P., 2001. *Azospirillum brasilense* and *Azospirillum lipoferum* hydrolyze conjugates of GA20 and metabolize the resultant aglycones to GA1 in seedlings of rice dwarf mutants. Plant Physiol. 125, 2053–2058.

Chandler, P.M., Marion-Poll, A., Ellis, M., Gubler, F., 2002. Mutants at the Slender1 locus of barley cv Himalaya. Molecular and physiological characterization. Plant Physiol. 129, 181–190.

Chaves, M.M., Maroco, J.P., Pereira, J.S., 2003. Understanding plant responses to drought - from genes to the whole plant. Funct. Plant Biol. 30, 239–264.

Clearwater, M., Lowe, R., Hofstee, B., Barclay, C., Mandemaker, A., Blattmann, P., 2004. Hydraulic conductance and rootstock effects in grafted vines of kiwifruit. J. Exp. Bot. 55, 1371–1382.

Clúa, A., Bottini, R., Brocchi, G.N., Bogino, J., Luna, V., Montaldi, E.R., 1996. Growth habit of *Lotus tenuis* shoots and the influence of photosynthetic photon flux density, sucrose and endogenous levels of gibberellins A1 and A3. Physiol. Plantarum 98, 381–388.

Cobelli, C., Carson, E., 2019. Introduction to Modelling in Physiology and Medicine, second ed. Academic Press, San Diego, USA.

Cookson, S.J., Ollat, N., 2013. Grafting with rootstocks induces extensive transcriptional re-programming in the shoot apical meristem of grapevine. BMC Plant Biol. 13, 147.

Cosgrove, D.J., 2005. Growth of the plant cell wall. Nat. Rev. Mol. Cell Biol. 6, 850–861.

Crozier, A., Kamiya, Y., Bishop, G., Yokota, T., 2000. Biosynthesis of hormones and elicitor molecules. In: Buchanan, B.B., Gruissem, W., Jones, R.L. (Eds.), Biochemistry and Molecular Biology of Plants, second ed. Am. Soc. Plant Physiol., Rockville, USA.

De Herralde, F., Alsina, M.M., Aranda, X., Save, R., Biel, C., 2006. Effects of rootstock and irrigation regime on hydraulic architecture of *Vitis vinifera* L. cv. Tempranillo. J. Int. Sci. Vigne Vin 40, 133–139.

Dhanoa, M., Lister, S., France, J., Barnes, R., 1999. Use of mean square prediction error analysis and reproducibility measures to study near infrared calibration equation performance. J. Near Infrared Spectrosc. 7, 133–143.

Di Filippo, M., Vila, H., 2011. Influence of different rootstocks on the vegetative and reproductive performance of *Vitis vinifera* L. Malbec under irrigated conditions. J. Int. Sci. Vigne Vin 45, 75–84.

Ehlert, C., Maurel, C., Tardieu, F., Simonneau, T., 2009. Aquaporin-mediated reduction in maize root hydraulic conductivity impacts cell turgor and leaf elongation even without changing transpiration. Plant Physiol. 150, 1093–1104.

Fan, Z.X., Zhang, S.B., Hao, G.Y., Ferry Slik, J., Cao, K.F., 2012. Hydraulic conductivity traits predict growth rates and adult stature of 40 Asian tropical tree species better than wood density. J. Ecol. 100, 732–741.

Farquhar, G.D., Sharkey, T.D., 1982. Stomatal conductance and photosynthesis. Annu. Rev. Plant Physiol. 33, 317–345.

Farquhar, G.D., von Caemmerer, S., Berry, J., 1980. A biochemical model of photosynthetic CO2 assimilation in leaves of C3 species. Planta 149, 78–90.

Fourcaud, T., Zhang, X., Stokes, A., Lambers, H., Körner, C., 2008. Plant growth modelling and applications: the increasing importance of plant architecture in growth models. Ann. Bot. 101, 1053–1063.

Gambetta, G.A., Manuck, C.M., Drucker, S.T., Shaghasi, T., Fort, K., Matthews, M.A., Walker, M.A., McElrone, A.J., 2012. The relationship between root hydraulics and scion vigour across *Vitis* rootstocks: what role do root aquaporins play? J. Exp. Bot. 63, 6445–6455.

Goshtasby, A.A., 2000. Grouping and parameterizing irregularly spaced points for curve fitting. ACM Trans. Graph. 19, 185–203.

Hedden, P., Sponsel, V., 2015. A century of gibberellin research. J. Plant Growth Regul. 34, 740–760.

Hooijdonk, V., Woolley, D., Warrington, I., Tustin, D., 2010. Initial alteration of scion architecture by dwarfing apple rootstocks may involve shoot-root-shoot signaling by auxin, gibberellin, and cytokinin. J. Hortic. Sci. Biotechnol. 85, 59–65.

Hsiao, T.C., 1990. Measurements of plant water status. Agron 30, 243–279.

Huerta, L., Forment, J., Gadea, J., Fagoaga, C., Pena, L., Perez-Amador, M.A., García-Martinez, J.L., 2008. Gene expression analysis in citrus reveals the role of gibberellins on photosynthesis and stress. Plant Cell Environ. 31, 1620–1633.

Hugalde, I., Bonada, M., Vila, H., 2018. The phenomenon of cavitation in grapevine… Unravelling implicated mechanisms. Rev. Fac. Cienc. Agrar. 50, 33–47.

Hugalde, I., Riaz, S., Agüero, C.B., Romero, N., Barrios-Masias, F., Nguyen, A.V., Vila, H., McElrone, A., Gómez Talquenca, S., Arancibia, C., Walker, M.A., 2017. Physiological and genetic control of vigour in a 'Ramsey' × 'Riparia Gloire de Montpellier' population. Acta Hortic. 1188, 205–212.

Ikeda, A., Ueguchi-Tanaka, M., Sonoda, Y., Kitano, H., Koshioka, M., Futsuhara, Y., Matsuoka, M., Yamaguchi, J., 2001. Slender rice, a constitutive gibberellin response mutant, is caused by a null mutation of the SLR1 gene, an ortholog of the height-regulating gene GAI/RGA/RHT/D8. Plant Cell 13, 999–1010.

Ingalls, B., 2013. Mathematical Modelling in Systems Biology: an Introduction. MIT Press, Cambridge, MA.

Jolliffe, I.T., Cadima, J., 2016. Principal component analysis: a review and recent developments. Phil. Trans. R. Soc. A. 37420150202.

Kaldenhoff, R., Grote, K., Zhu, J.J., Zimmermann, U., 1998. Significance of plasmalemma aquaporins for water-transport in *Arabidopsis thaliana*. Plant J. 14, 121–128.

Karavin, N., 2014. Effects of leaf and plant age on specific leaf area in deciduous tree species *Quercus cerris* L. var. Cerris. Bangl. J. Bot. 42, 301–306.

Kobayashi, M., Gaskin, P., Spray, C., Phinney, B., Mac Millan, J., 1994. The metabolism of gibberellin A20 to gibberellin A1 by tall and dwarf mutants of *Oryza sativa* and *Arabidopsis thaliana*. Plant Physiol. 106, 1367–1372.

Kopcewicz, J., 1968. Seasonal changes of gibberellin-like substances and growth inhibitors in the apical meristems of Pine (*Pinus sylvestris* L.). Acta Soc. Bot. Pol. 37, 579–587.

Lambers, H., Chapin III, F.S., Pons, T.L., 2008. Growth and allocation. In: Lambers, H., Chapin, F.S., Pons, T.L. (Eds.), Plant Physiological Ecology, second ed. Springer-Verlag, New York, USA.

Lambers, H., Nagel, O.W., Van Arendonk, J., 1995. The control of biomass partitioning in plants from "favourable" and "stressful" environments: a role for gibberellins and cytokinins. Bulg. J. Plant Physiol. 21, 24–32.

Li, H., Ralph, P.L., 2018. Local PCA shows how the effect of population structure differs along the genome. Genetics 11 (1).

Li, J., Yu, K., Wei, J., Ma, Q., Wang, B., Yu, D., 2010. Gibberellin retards chlorophyll degradation during senescence of *Paris polyphylla*. Biol. Plantarum 54, 395–399.

Lovisolo, C., Perrone, I., Carra, A., Ferrandino, A., Flexas, J., Medrano, H., Schubert, A., 2010. Drought-induced changes in development and function of grapevine (*Vitis* spp.) organs and in their hydraulic and non-hydraulic interactions at the whole-plant level: a physiological and molecular update. Funct. Plant Biol. 37, 98–116.

Lovisolo, C., Tramontini, S., Flexas, J., Schubert, A., 2008. Mercurial inhibition of root hydraulic conductance in *Vitis* spp. rootstocks under water stress. Environ. Exp. Bot. 63, 178–182.

Lowe, K., Walker, M., 2006. Genetic linkage map of the interspecific grape rootstock cross Ramsey (*Vitis champinii*) × Riparia Gloire (*Vitis riparia*). Theor. Appl. Genet. 112, 1582–1592.

Magni, P., Sparacino, G., 2014. Parameter estimation. In: Modelling Methodology for Physiology and Medicine. Ewart Carson, Claudio Cobelli, second ed. Elsevier. London.

Marguerit, E., Brendel, O., Lebon, E., Van Leeuwen, C., Ollat, N., 2012. Rootstock control of scion transpiration and its acclimation to water deficit are controlled by different genes. New Phytol. 194, 416–429.

Miele, A., Rizzon, L.A., 2017. Rootstock-scion interaction: 2. Effect on the composition of Cabernet Sauvignon grape must. Rev. Bras. Frutic. 39 (3), 434.

Moreno, D., Berli, F.J., Piccoli, P.N., Bottini, R., 2011. Gibberellins and abscisic acid promote carbon allocation in roots and berries of grapevines. J. Plant Growth Regul. 30, 220–228.

Muangprom, A., Osborn, T., 2004. Characterization of a dwarf gene in *Brassica rapa*, including the identification of a candidate gene. Theor. Appl. Genet. 108, 1378–1384.

Murcia, G., Pontin, M., Reinoso, H., Baraldi, R., Bertazza, G., Gómez-Talquenca, S., Bottini, R., Piccoli, P.N., 2016. ABA and GA3 increase carbon allocation in different organs of grapevine plants by inducing accumulation of non-structural carbohydrates in leaves, enhancement of phloem area and expression of sugar transporters. Physiol. Plantarum 156, 323–337.

Nouvellon, Y., Laclau, J.-P., Epron, D., Kinana, A., Mabiala, A., Roupsard, O., Bonnefond, J.M., Le Maire, G., Marsden, C., Bontemps, J.-D., 2010. Within-stand and seasonal variations of specific leaf area in a clonal *Eucalyptus* plantation in the Republic of Congo. For. Ecol. Manag. 259, 1796–1807.

Ollat, N., Tandonnet, J., Bordenave, L., Decroocq, S., Geny, L., Gaudillere, J., Fouquet, R., Barrieu, F., Hamdi, S., 2003. Vigour conferred by rootstock: hypotheses and direction for research. Bulletin de l'OIV, Paris 76, 581–595.

Pallas, B., Loi, C., Christophe, A., Cournède, P.H., Lecoeur, J., 2010. Comparison of three approaches to model grapevine organogenesis in conditions of fluctuating temperature, solar radiation and soil water content. Ann Bot-London 107, 729–745.

Peccoux, A., Loveys, B., Zhu, J., Gambetta, G.A., Delrot, S., Vivin, P., Schults, H.R., Ollat, N., Dai, Z., 2018. Dissecting the rootstock control of scion transpiration using model-assisted analyses in grapevine. Tree Physiol. 38, 1026–1040.

Piccoli, P., Lucangeli, D., Schneider, G., Bottini, R., 1997. Hydrolysis of [17,17-2H2] gibberellin A20-glucoside and [17,17-2H2]gibberellin A20 -glucosyl ester by *Azospirillum lipoferum* cultured in a nitrogen free biotin-based chemically-defined medium. Plant Growth Regul. 23, 179–182.

Pleban, J.R., Guadagno, C.R., Mackay, D.S., Weinig, C., Ewers, B.E., 2020. Rapid chlorophyll a fluorescence light response curves mechanistically inform photosynthesis modeling. Plant Physiol.

Polymenis, M., Schmidt, E.V., 1997. Coupling of cell division to cell growth by translational control of the G1 cyclin CLN3 in yeast. Genes Dev. 11, 2522–2531.

Pou, A., Medrano, H., Flexas, J., Tyerman, S.D., 2013. A putative role for TIP and PIP aquaporins in dynamics of leaf hydraulic and stomatal conductances in grapevine under water stress and re-watering. Plant Cell Environ. 36, 828–843.

Pury, D.D., Farquhar, G., 1997. Simple scaling of photosynthesis from leaves to canopies without the errors of big-leaf models. Plant Cell Environ. 20, 537–557.

Rebolledo, M., Dingkuhn, M., Courtois, B., Gibon, Y., Clément-Vidal, A., Cruz, D.F., Duitama, J., Lorieux, M., Luquet, D., 2015. Phenotypic and genetic dissection of component traits for early vigour in rice using plant growth modelling, sugar content analyses and association mapping. J. Exp. Bot. 66, 5555–5566.

Reich, P., Ellsworth, D., Walters, M., 1998. Leaf structure (specific leaf area) modulates photosynthesis–nitrogen relations: evidence from within and across species and functional groups. Funct. Ecol. 12, 948–958.

Rogiers, S.Y., Greer, D.H., Hatfield, J.M., Hutton, R.J., Clarke, S.J., Hutchinson, P.A., Somers, A., 2012. Stomatal response of an anisohydric grapevine cultivar to evaporative demand, available soil moisture and abscisic acid. Tree Physiol. 32, 249–261.

Rood, S.B., Buzzell, R.I., Mander, L.N., Pearce, D., Pharis, R.P., 1988. Gibberellins: a phytohormonal basis for heterosis in maize. Science 241, 1216–1218.

Salisbury, F., Ross, C., 2000. Fisiología de las plantas 1. Células: agua, soluciones y superficies. International Thomson Editores Madrid, Spain.

Schmidt, D., Bahr, C., Friedel, M., Kahlen, K., 2019. Modelling approach for predicting the impact of changing temperature conditions on grapevine canopy architectures. Agron 9, 426.

Šimura, J., Antoniadi, I., Široká, J., Tarkowská, D., Strnad, M., Ljung, K., Novák, O., 2018. Plant Hormonomics: multiple phytohormone profiling by targeted metabolomics. Plant Physiol. 177, 476–489.

Sivasakthi, K., Tharanya, M., Kholová, J., Wangari Muriuki, R., Thirunalasundari, T., Vadez, V., 2017. Chickpea genotypes contrasting for vigor and canopy conductance also differ in their dependence on different water transport pathways. Front. Plant Sci. 8, 1663.

Syvertsen, J., Graham, J., 1985. Hydraulic conductivity of roots, mineral nutrition, and leaf gas exchange of citrus rootstocks. J. Am. Soc. Hortic. Sci. 110, 865–869.

Taiz, L., Zeiger, E., Møller, I.M., Murphy, A., 2015. Plant Physiology and Development, sixth ed. Sinauer Associates Inc, Sunderland Massachusetts, USA.

Talbott, L.D., Zeiger, E., 1996. Central roles for potassium and sucrose in guard-cell osmoregulation. Plant Physiol. 111, 1051–1057.

Talbott, L.D., Zeiger, E., 1998. The role of sucrose in guard cell osmoregulation. J. Exp. Bot. 49, 329–337.

Tandonnet, J.P., Cookson, S.J., Vivin, P., Ollat, N., 2010. Scion genotype controls biomass allocation and root development in grafted grapevine. Aust. J. Grape Wine Res. 16, 290–300.

Tardieu, F., Simonneau, T., 1998. Variability among species of stomatal control under fluctuating soil water status and evaporative demand: modelling isohydric and anisohydric behaviours. J. Exp. Bot. 49, 419–432.

Ubeda-Tomás, S., Federici, F., Casimiro, I., Beemster, G.T., Bhalerao, R., Swarup, R., Doerner, P., Haseloff, J., Bennett, M.J., 2009. Gibberellin signaling in the endodermis controls *Arabidopsis* root meristem size. Curr. Biol. 19, 1194–1199.

Vandeleur, R.K., Mayo, G., Shelden, M.C., Gilliham, M., Kaiser, B.N., Tyerman, S.D., 2009. The role of plasma membrane intrinsic protein aquaporins in water transport through roots: diurnal and drought stress responses reveal different strategies between isohydric and anisohydric cultivars of grapevine. Plant Physiol. 149, 445–460.

Wong, S., Cowan, I., Farquhar, G.D., 1979. Stomatal conductance correlates with photosynthetic capacity. Nature 282, 424–426.

Wu, A., Song, Y., Van Oosterom, E.J., Hammer, G.L., 2016. Connecting biochemical photosynthesis models with crop models to support crop improvement. Front. Plant Sci. 7, 1518.

Yamaguchi, S., 2008. Gibberellin metabolism and its regulation. Annu. Rev. Plant Biol. 59, 225–251.

Yin, X., Struik, P., 2009. C 3 and C 4 photosynthesis models: an overview from the perspective of crop modelling. NJAS - Wageningen J. Life Sci. 57, 27–38.

Yörük, I., Türker, M., Battal, P., Kazankaya, A., Tileklioğlu, B., 2004. Seasonal changes of endogenous plant hormones in *Rosa canina*. Acta Hortic. 690, 199–202.

Zhu, J., Dai, Z., Vivin, P., Gambetta, G.A., Henke, M., Peccoux, A., Ollat, N., Delrot, S., 2018. A 3-D functional–structural grapevine model that couples the dynamics of water transport with leaf gas exchange. Ann. Bot. (Lond.) 121, 833–848.

Zhu, J., Génard, M., Poni, S., Gambetta, G.A., Vivin, P., Vercambre, G., Dai, Z., 2019. Modelling grape growth in relation to whole-plant carbon and water fluxes. J. Exp. Bot. 70, 2505–2521.

Zorić, L., Ljubojević, M., Merkulov, L., Luković, J., Ognjanov, V., 2012. Anatomical characteristics of cherry rootstocks as possible preselecting tools for prediction of tree vigour. J. Plant Growth Regul. 31, 320–331.

Zufferey, V., Smart, D., 2012. Stomatal behaviour of irrigated *Vitis vinifera* cv. Syrah following partial root removal. Funct. Plant Biol. 39, 1019–1027.